Microtubule-based nuclear movement occurs independently of centrosome positioning in migrating neurons

Hiroki Umeshima*†, Tomoo Hirano†, and Mineko Kengaku*‡

*Laboratory for Neural Cell Polarity, RIKEN Brain Science Institute, 2-1 Hirosawa, Wako, Saitama 351-0198, Japan; and †Department of Biophysics, Graduate School of Science, Kyoto University, Kyoto 606-8502, Japan

Communicated by Clifford J. Tabin, Harvard Medical School, Boston, MA, August 27, 2007 (received for review June 15, 2007)

During neuronal migration in the developing brain, it is thought that the centrosome precedes the nucleus and provides a cue for nuclear migration along the microtubules. In time-lapse imaging studies of radially migrating granule cells in mouse cerebellar slices, we observed that the movements of the nucleus and centrosome appeared to occur independently of each other. The nucleus often migrated ahead of the centrosome during its saltatory movement, negating the supposed role of the centrosome in pulling the nucleus. The nucleus was associated with dynamic microtubules enveloping the entire nucleus and stable microtubules extending from the leading process to the anterior part of the nucleus. Neither of these perinuclear microtubules converged at the centrosome. Disruption or excess formation of stable microtubules attenuated nuclear migration, indicating that the configuration of stable microtubules is crucial for nuclear migration. The inhibition of LIS1 function, a regulator of a microtubule motor dynein, specifically blocks nuclear migration without affecting the coupling of the centrosome and microtubules in the leading process, suggesting that movements of the nucleus and centrosome are differentially regulated by dynein motor function. Thus, the nucleus moves along the microtubules independently of the position of the centrosome in migrating neurons.

neuronal migration | nucleus | LIS1 | acetylated tubulin | tyrosinated tubulin

Neurons in the vertebrate brain migrate from the site of birth to their final points of integration into specific neural circuits. Migrating neurons are polarized with their leading processes extended in the direction of movement. Subsequently, their cell bodies containing the nucleus and other organella are translocated into the leading process (1–3). The mechanism of nuclear movement in migrating neurons is clearly distinct from other cell types: unlike fibroblastic cells in which the forward displacement of the nucleus tightly follows the actin-dependent extension of the leading edge (4), nuclear movement in neurons is not directly triggered by the leading process extension (2, 5). Instead, the centrosome is considered to play a key role in driving nuclear migration in neurons. The centrosome typically precedes and is coupled to the nucleus via perinuclear microtubules that envelop and capture the nucleus (6–11). Current models suggest that the centrosome first moves into the leading process and serves as a cue for forward displacement of the nucleus along the microtubules (7, 8, 12–14). To better understand the mechanism of nuclear migration in neurons, we performed direct imaging of radial migration of granule cells in organotypic slices of developing mouse cerebellum in which the environment closely resembles that found *in vivo*. We demonstrate that the nucleus migrates along microtubules toward the leading process independently of the centrosome.

Results

Large-Amplitude Saltatory Movements of the Nucleus in Radially Migrating Granule Cells. To observe the nuclei of migrating granule cells, the external granule layer of P8 mice were coelectroporated with plasmid vectors containing EGFP and a DsRed2 variant red fluorescent protein conjugated with nuclear localization signals (DsRed2-Nuc). Coronal sections (300 μm) of the cerebellar vermis were made 48 h after *in vivo* electroporation and observed under time-lapse confocal microscopy. Most of the labeled cells were identified as granule cells undergoing radial migration with a thick leading process oriented toward the internal granule layer [see supporting information (SI) Fig. 7 and SI Movie 1] (5, 15, 16). The soma was filled with the nucleus, which was delineated by a thin ring of cytoplasm (Fig. 1*A*). During radial migration in the molecular layer (ML), granule cells typically exhibited saltatory nuclear movements with alternate resting (or slow-moving) and fast-moving phases (Fig. 1 *A* and *C*; see also SI Movie 2) (2, 17). The average speed in the ML (17.1 ± 2.4 μm/h; mean ± SEM; n = 15 cells) and the speed in the fast-moving phase (54.8 ± 4.6 μm/h; n = 18 cells) were comparable to those reported in previous studies. During resting (slow-moving) phases, the nucleus was stationary or moved at 29.1 μm/h or less. The duration of a resting phase varied greatly between 3 and 129 min (average 41.1 ± 6.4 min; n = 26 cells). In fast-moving phases, the nucleus was observed to advance rapidly into the leading process, with amplitudes markedly greater than that observed in dissociated cultures [10.9 ± 0.9 μm; n = 18 cells, compared with 1.3 μm in dissociated cells (7)]. These observations indicate that radial migration of granule cells *in situ* is much more dynamic than in dissociated cultures. The leading process with a tiny growth cone was continuously extended regardless of the nuclear movement, supporting their mutual independence in neurons (2, 5). The centrosome-containing dilation observed in the leading processes of migrating cortical interneurons and subventricular zone (SVZ) cells was only occasionally found in granule cells (12, 18). The shape of the nucleus changed dynamically depending on the migration phase; it elongated in the direction of the movement at the onset of moving phases and became round during resting phases (Fig. 1*B* and SI Movie 2). The correlation between the movement and shape of the nucleus suggests dynamic regulation of the force driving the nuclear movement.

The Nucleus Migrates Past the Centrosome. The centrosome has been shown to precede nuclear migration in several types of neurons (7–10, 12, 18). To analyze the dynamic behavior of the

Author contributions: H.U. and M.K. designed research; H.U. performed research; H.U. analyzed data; and T.H. and M.K. wrote the paper.

The authors declare no conflict of interest.

Freely available online through the PNAS open access option.

Abbreviations: ML, molecular layer; SVZ, subventricular zone; tyr-tubulin, tyrosinated tubulin; Ac-tubulin, acetylated tubulin.

‡To whom correspondence should be addressed. E-mail: kengaku@brain.riken.jp.

This article contains supporting information online at www.pnas.org/cgi/content/full/0708047104/DC1.

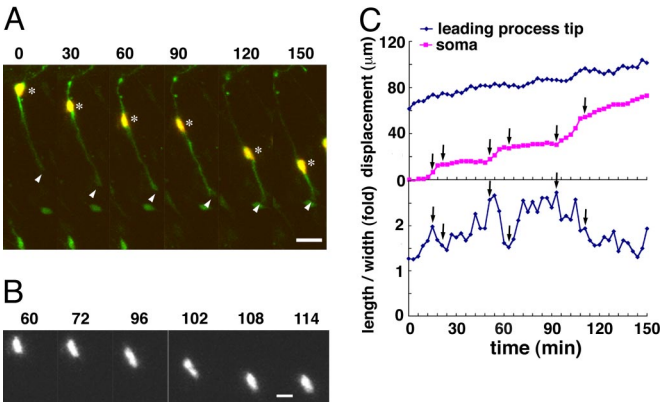

Fig. 1. Saltatory movements of the nucleus occur independently of leading process extension in radial migration of granule cells. (*A*) Time-lapse sequence of granule cells undergoing radial migration in the ML in P10 mouse cerebella shown in SI Movie 2. Cells were coelectroporated with pCAG-EGFP and pCAG-DsRed2-Nuc to visualize the cell morphology (green) and nucleus (red), respectively. Coronal slices were made 48 h after *in vivo* electroporation and imaged every 3 min. Asterisks and arrowheads indicate nuclei and leading process tips, respectively. Times in all time-lapse images are indicated in minutes. Panels are oriented pial side up, with white matter side down. (*B*) Imaging of the nucleus of the neuron shown in *A* at different time points. (*C*) Positions of the leading process tip (blue in *Upper*) and approximated oval center of the nucleus (magenta in *Upper*) and the length/width ratio of the nucleus (*Lower*) in neurons shown in *A* plotted against time. Nuclear migration consists of clear fast-moving and resting (slow-moving) phases, whereas leading process extension is relatively constant. The length/width ratio (the ratio of nuclear diameter along the leading and trailing poles relative to diameter along perpendicular axis) roughly correlated with the nuclear translocation and increased at the onset of the fast moving phases (arrows). (Scale bars: 20 μm, *A*; 10 μm, *B*.)

centrosome during migration, granule cells were coelectroporated with DsRed-Express and GFP-tagged Centrin2 (8). We first confirmed that Centrin2-GFP signals were specifically localized to the centrosomal structures (SI Fig. 8). The centrosome was predominantly observed in front of the soma in the outermost ML (Fig. 2*A*; at time point 0). Two centrioles were occasionally separated from each other as observed in tangentially migrating interneurons (Fig. 2*A Lower*) (18). In some of the migrating cells, the centrosome maintained a position ahead of the soma during saltatory movements within the ML consistent with previous reports (data not shown) (7, 8, 12, 18). Unexpectedly, we found that in majority of the cells the soma rapidly advanced past the centrosome (13 of 18 cells observed; Fig. 2 and SI Movies 3 and 4). During the two-step movement of the soma, the centrosome advanced at a constant speed comparable with that of the leading process extension. The soma moved faster than the centrosome during moving phases, resulting in the centrosome being left behind in a stepwise manner after several cycles of somal movement (Fig. 2*B*). The centrosome would then revert to an advanced position during long resting phases of the soma.

To analyze the relative position of the centrosome and nucleus, tissues were fixed and labeled with DAPI nuclear stain. Granule cell soma demarcated by DsRed-Express was almost fully occupied by the nucleus and contained little cytoplasm consistent with previous reports (8) and our time-lapse images in Fig. 1 (Fig. 3*A*). Centrin2-positive centrosomes were most commonly observed in the leading process within 5 μm from the nucleus at a mean distance 0.7 $\pm$ 2.9 μm in migrating neurons (Fig. 3*B*; mean $\pm$ SD; $n = 96$ cells). Thus, in contrast to tangentially migrating cortical interneurons and SVZ neuroblasts in which the long-distance forward migration of the centrosome precedes each nuclear migration (12, 18), the forward movement of the centrosome was apparently smaller than the amplitude of nuclear movements in granule cells. Furthermore, the centrosome was often located in the cytoplasm between the leading and trailing poles of the nucleus (Fig. 3 *A′* and *B*; 35.4%; $n = 96$ cells). We also analyzed the localization of the Golgi apparatus, as it has been shown to associate tightly with the centrosome (Fig. 3 *C* and *C′*) (18, 19). The Golgi apparatus was observed behind the leading pole of the nucleus in 9 of 30 migrating granule cells in the ML (the Golgi apparatus was entirely behind the leading pole in six cells and partially over-

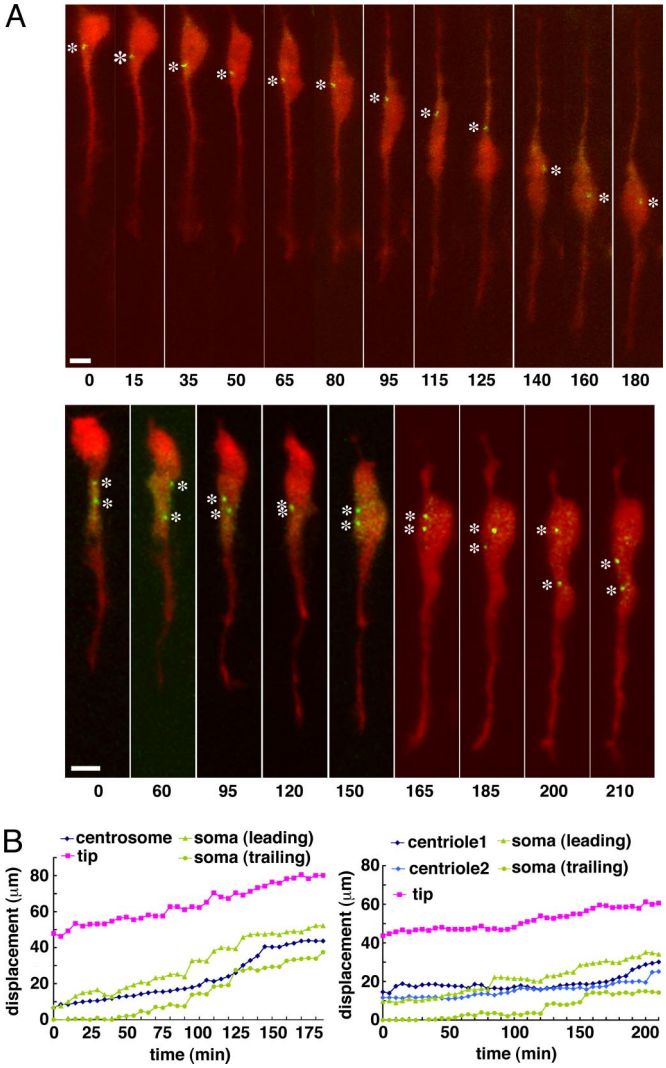

Fig. 2. The soma translocates past the centrosome toward the leading process during radial migration of granule cells. (*A*) Time-lapse laser-confocal images of granule cells (Cell 1, *Upper*; Cell 2, *Lower*) in the ML transduced with pCAG-DsRed-Express and pCentrin2-GFP (5-min intervals; see also SI Movies 3 and 4). Times are indicated in minutes. Panels are oriented pial side up. Centrosomes labeled with Centrin2-GFP (green) indicated by asterisks were mostly located ahead of the soma in the direction of migration in the outer ML (time point 0). The two centrioles were occasionally observed separated from each other (*Lower*). Long, saltatory movements of the soma surpassed the centrosome (*Upper*) or both centrioles (*Lower*). (Scale bars: 5 μm.) (*B*) Graphs of the positions of the leading process tip (magenta), centrosome (dark and light blue), and the leading and trailing poles of the soma (green) of neurons shown in *A* plotted against time. (*Left*) Cell 1. (*Right*) Cell 2. The nucleus migrated past the centrosome until the centrosome reached the rear pole of the soma after serial nuclear movements. The centrosome moved at a constant speed comparable to the leading process extension, then advanced rapidly to the front when it reached the cell rear.

DEVELOPMENTAL BIOLOGY

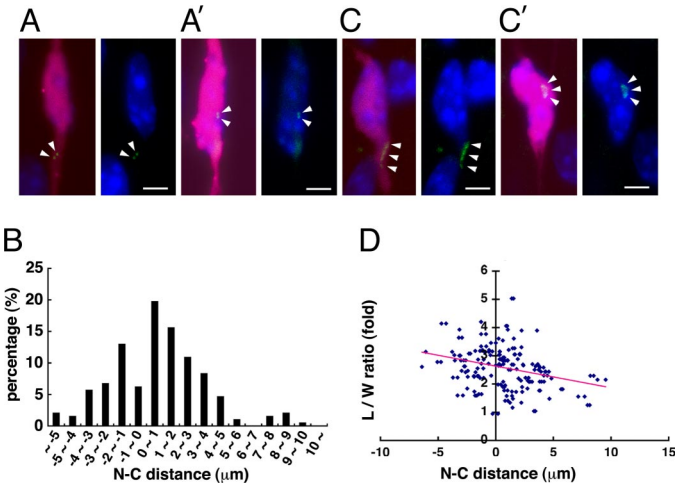

Fig. 3. Localization of the centrosome and Golgi apparatus in migrating granule cells in the ML. (*A* and *A′*) Visualization of centrosomes in granule cells coelectroporated with DsRed-Express (pseudocolored in magenta) and Centrin2-GFP (green), then sectioned and stained with DAPI (blue). Centrosomes were positioned either in front of the nucleus (*A*) or within the soma (*A′*). (*B*) Histogram of the positions of the centrosomes within migrating granule cells. The distances (micrometers) from the leading pole of the nucleus (point 0) to the leading process (plus; right) and the soma (minus; left) are represented along the *x* axis and the percentages of total neuron number in each bin is represented along the *y* axis. Significant numbers of centrosomes were observed behind the leading poles of the nuclei. (*C* and *C′*) Visualization of the Golgi apparatus in granule cells transduced with DsRed-Express, then immunostained with anti-GM130. The Golgi apparatus in some cells was positioned ahead of the nucleus (*C*), whereas others were localized within the soma (*C′*). (*D*) Correlation of centrosomal position and nuclear shape. The centrosomal position measured in *B* relative to the length/width ratio of the nucleus is shown. The length/width ratio was calculated as described in Fig. 1. The solid line represents linear regression ($r^2 = 0.087$). (Scale bars: 5 μm.)

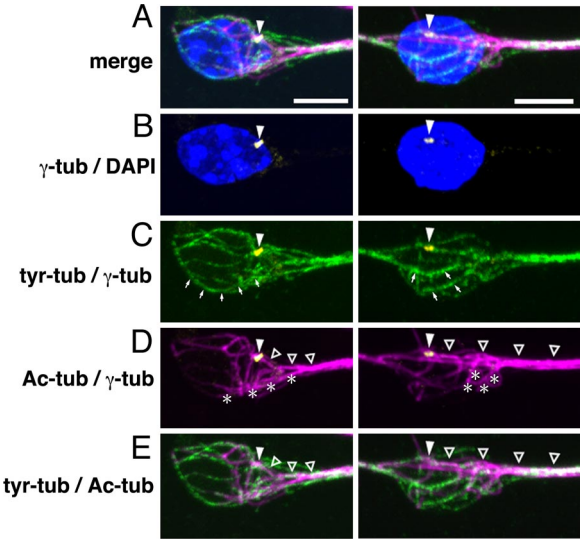

Fig. 4. The microtubule cytoskeleton of migrating granule cells. (*Left*) Cell 1. (*Right*) Cell 2. Granule cells in cerebellar reaggregate cultures were multiply stained for γ-tubulin (pseudocolored in yellow), tyr-tubulin (green), Ac-tubulin (magenta), and DAPI (blue). Panels are oriented with the forward direction of migration (distal side of the explant) to the right, and backward (proximal side) to the left. (*A*) Merged view. (*B*) Immunostaining for γ-tubulin showed that the centrosome (arrowheads) was located in front of the nucleus (*Left*) or within the soma (*Right*). (*C*) Dynamic microtubules rich in tyr-tubulin form the perinuclear microtubule cage. Some of the microtubule filaments appeared not to converge at the centrosome (arrows). (*D*) Stable microtubules rich in Ac-tubulin form a whisk-like structure at the anterior surface of the nucleus. The stable perinuclear microtubules extend from the leading process independent of the centrosome (asterisks). Thick bundles of stable microtubules in the leading process (open arrowheads) were converged at the centrosome whether it was located ahead or behind the anterior pole of the nucleus. (*E*) Merged view of *C* and *D*. (Scale bars: 5 μm.)

lapped with the nucleus in three cells), supporting the rear positioning of the centrosome. The centrosome and Golgi apparatus tended to localize behind nuclei that were elongated along the radial axis rather than rounded nuclei, suggesting that the centrosome positioned behind the leading pole of the nucleus during moving phases, whereas it positioned ahead during long resting phases (Fig. 3*D*). From these data, we conclude that the centrosome does not maintain a position in front of the nucleus nor serves as a target for nuclear displacement during radial migration of granule cells.

Perinuclear Microtubules Do Not Converge at the Centrosome. Previous studies have indicated that microtubules radiating from the centrosome are anchored to the leading process and nucleus. The centrosome is thought to relay the force generated by leading process extension to the nucleus via the microtubule bundles (13, 20). We thus analyzed the microtubule cytoskeleton in migrating granule cells in a reaggregate culture of external granule layer cells (16). We first confirmed that somal migration over the centrosome was reconstituted in the reaggregate culture (SI Movie 5). Consistently, γ-tubulin-positive centrosomes were positioned within or ahead of the nucleus in fixed granule cells in culture (arrowheads in Fig. 4 *A* and *B*; 43% within the cell body, *Right* and 57% ahead of the nucleus, *Left*; $n = 221$ cells). We next monitored tyrosination and acetylation states of α-tubulin as indirect indicators of microtubule dynamics (Fig. 4 *C–E*). Tyrosinated tubulin (tyr-tubulin) is enriched in dynamic microtubule polymers, whereas acetylated tubulin (Ac-tubulin) accumulates in stable microtubule configurations (21–24). We confirmed the presence of previously observed cage-like structures around the nucleus and thick bundles extending into the leading process (6, 7). The microtubule bundles in the leading process were rich in both tyr- and Ac-tubulin. The proximal ends of the microtubule bundles toward the leading process appeared to converge at the centrosome whether it was located within or ahead of the nucleus (open arrowheads in Fig. 4 *D* and *E*). In contrast, the perinuclear microtubule cage consists of dynamic tyr-tubulin but is almost deficient in Ac-tubulin (Fig. 4 *C–E*). Some of the perinuclear microtubules were apparently diverged from the centrosome (arrows in Fig. 4*C*). Besides these structures, we often observed whisk-like structures of microtubule filaments rich in Ac-tubulin that extended from the leading process toward the anterior surface of the nucleus (asterisks in Fig. 4*D*). In contrast to the tyrosinated, nonacetylated microtubule cage enveloping the entire surface of the nucleus, acetylated microtubules were polarized to cover only the anterior part of the nucleus. These perinuclear acetylated microtubules appeared to extend toward the leading process independent of the centrosome. Thus, neither of the microtubule structures associated with the nucleus converged at the centrosome.

To explore the significance of microtubule organization in nuclear migration, we applied a microtubule-disrupting agent, nocodazole, to migrating neurons in culture. Nocodazole treatment at 1 μM had little effect on nuclear movement as was previously reported with SVZ neurons (12). Although the number of migrating cells slightly decreased, the speed of nuclear movement was not changed in most cells after the addition of nocodazole (Fig. 5 *A–C* and SI Movie 6; 21.3 ± 1.2 μm/h, $n =$ 88 cells, DMSO vs. 18.9 ± 1.8 μm/h, $n = 84$ cells, nocodazole, from three experiments; mean ± SEM; Student's *t* test, $P >$ 0.25). As nocodazole has differential dose-dependent effects on

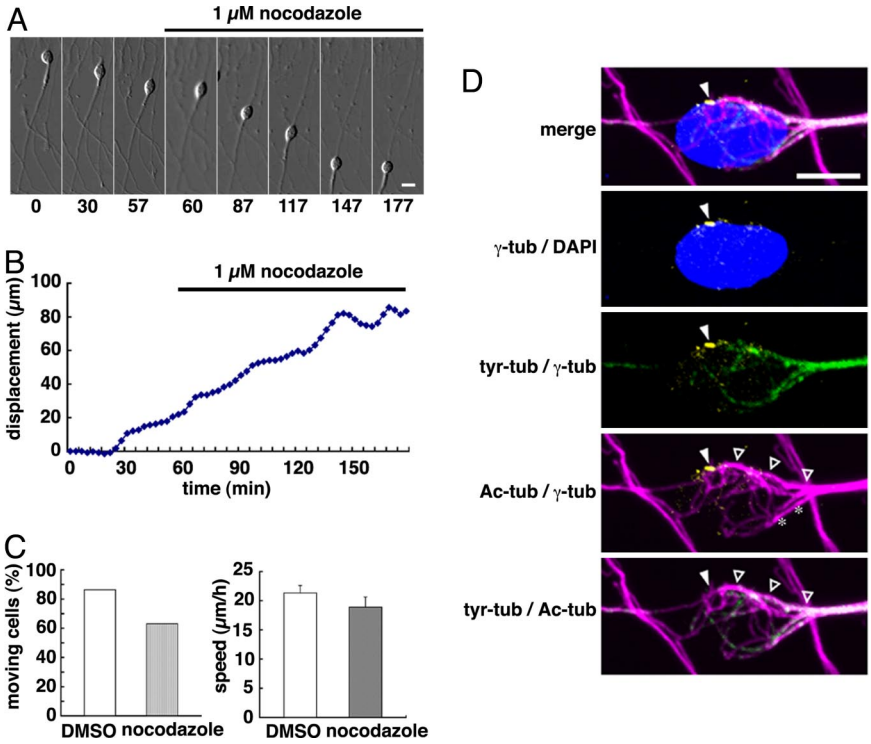

Fig. 5. The stable microtubules are sufficient for driving nuclear migration. (*A*) The application of 1 μM nocodazole did not inhibit granule cell migration in a reaggregate culture (see also SI Movie 6). Times in all time-lapse images are indicated in minutes. (*B*) Graphs indicate the positions of the cell body of the neuron shown in *A* plotted against time. Nocodazole was added at 60 min. (*C*) Percentage of migrating cells that moved >20 μm in 2 h (*Left*) and the average speed (*Right*) after treatment with DMSO (control) or nocodazole. (*D*) The addition of 1 μM nocodazole selectively disrupted dynamic microtubules. Perinuclear microtubule cages consisting of tyr-tubulin (green) were scarcely formed, whereas Ac-tubulin-positive stable microtubules (magenta) that were associated with the anterior half of the nucleus (asterisks) and those linked to the centrosome (open arrowheads) remained intact. Filled arrowheads indicate the position of centrosome. Panels are oriented with the forward direction of migration to the right. (Scale bars: 10 μm, *A*; 5 μm, *D*.)

stable and dynamic microtubules (25, 26), we examined the microtubule structures in neurons treated with 1 μM nocodazole. The perinuclear microtubule cage, which is rich in tyr-tubulin and deficient in Ac-tubulin, mostly disappeared. In contrast, the stable microtubules consisting of both tyr- and Ac-tubulin remained intact, including whisk-like filaments associated with the anterior part of the nucleus (Fig. 5*D*). These results suggest that the forward movement of the nucleus takes place in the absence of the microtubule cage consisting of dynamic microtubules.

When the nocodazole dose was raised to 10 μM, granule cells immediately lost their bipolar morphology and ceased forward movement. The leading process rapidly shrank, and the cell body was flattened and agitated in random orientations (SI Fig. 9*A* and SI Movie 7). At 10 μM, the polarized arrangement of the nucleus-associated microtubules was completely disrupted (SI Fig. 9*B*). Excess formation of stable microtubules also inhibited somal migration. Treatment with a microtubule-stabilizing agent, taxol (1 μM), halted or slowed the movement of the cell bodies, whereas leading processes appeared to be relatively unaffected (SI Fig. 9 *C* and *D* and SI Movie 8). Perinuclear cages were highly acetylated and stabilized in taxol-treated cells, resulting in excess formation of stable microtubules on the posterior side of the nucleus (SI Fig. 9*E*).

Taken together, these results suggest that the dynamic microtubule cage is dispensable, whereas the polarized arrangement of stable microtubules extending from the leading process toward the anterior part of the nucleus is crucial for nuclear migration in granule cells (SI Fig. 10 *A* and *B*).

LIS1/Dynein Complex Is Differentially Involved in Nuclear and Centrosomal Migration. We next analyzed the function of the microtubule-dependent motor dynein and its important binding partner, LIS1, in nuclear migration in neurons. It has been shown that loss of dynein or LIS1 function disrupts the coupling of the nucleus and centrosome and nuclear migration in neurons (8, 27–29). Consistent with previous reports, overexpression of a N-terminal fragment of LIS1, which has a dominant inhibitory effect on dynein function (LIS1N), significantly inhibited the radial migration of granule cells (Fig. 6*A* and *B* and SI Movie 9) (28, 30). Soma remained oval in shape without periodical stretching and rarely underwent long jumps, indicating that nuclear migration was impaired by LIS1 dysfunction. In contrast, the leading process was abnormally elongated, demonstrating that the leading process extension persists in the absence of nuclear migration (28, 31). Overexpression of dynamitin, which disassembles the dynein motor complex component dynactin, basically showed the same phenotype (SI Fig. 11*A*) (8, 28, 32). Consistent with previous reports, centrosomes were often well separated from the nuclei within the long leading process and moved independently of the nuclei in the absence of LIS1 function in brain slices (SI Fig. 11 *B* and *C* and SI Movie 10). Statistical analysis on fixed tissue preparations revealed that the distance between the centrosome and nucleus increased with greater variability (Fig. 6 *C* and *D*; 0.7 ± 2.9 μm, $n = 96$ cells, control vs. 4.4 ± 4.3 μm, $n = 56$ cells, LIS1N; mean ± SD; Student's *t* test, $P < 0.01$). In addition, the number of cells with centrosomes located behind the leading pole of the nuclei was significantly decreased, implying the inhibition of nuclear migration past the centrosome (Fig. 6*D*; nucleus–centrosome distance <0; 10.7% in cells expressing LIS1N vs. 35.4% in control). In granule cells overexpressing LIS1N in reaggregate cultures, the centrosome traveled separately from the nucleus in close association with microtubule bundles toward the leading process, suggesting that the coupling of the centrosome and leading process is independent of

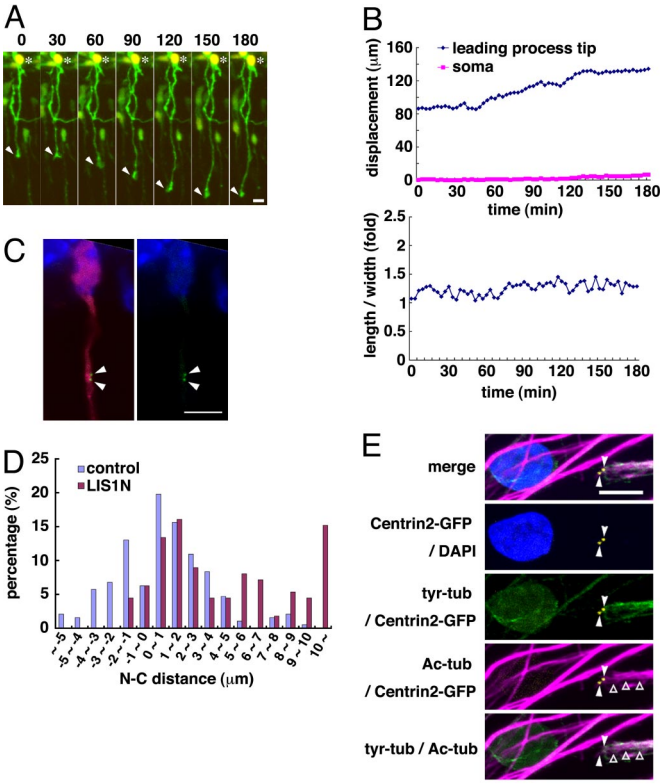

Fig. 6. Inhibition of LIS1 disrupts nuclear migration but not centrosome migration in granule cells. (*A*) Time-lapse laser-confocal images of granule cells in cerebellar slice transduced with LIS1N, pCAG-EGFP, and pCAG-DsRed2-Nuc (see SI Movie 9). Times are indicated in minutes. (*B*) Positions of the leading process tip (blue in *Upper*) and approximated oval center of the nucleus (magenta in *Upper*) and the length/width ratio of the nucleus (*Lower*) in neurons shown in *A* plotted against time. Nuclear migration is inhibited, whereas constant extension of the leading process is not affected. Periodical stretching of the nucleus is not seen. (*C*) Positions of the centrosome and nucleus in granule cells overexpressing LIS1N. Granule cells were transduced with DsRed-Express (pseudocolored in magenta), LIS1N, and Centrin2-GFP (green), and then sectioned and stained with DAPI (blue) 48 h after electroporation. (*D*) Histogram of the position of the centrosome in control (blue) and LIS1N-expressing granule cells (magenta). LIS1 inhibition increased the nucleus–centrosome distance, indicated by a rightward shift in the bin distribution. (*E*) LIS1 inhibition did not affect the coupling of the centrosome and leading process. Granule cells in a reaggregate culture were cotransduced with Centrin2-GFP (yellow) and LIS1N and stained for tyr-tubulin (green), Ac-tubulin (magenta), and DAPI (blue). Panels are oriented with the forward direction of migration to the right. The stable microtubule bundles in the leading process (open arrowheads) were tightly associated with the centrosome far ahead of the nucleus (filled arrowheads). Because LIS1-deficient cells failed to travel a long distance from the explant, bundles of Ac-tubulin derived from leading processes of other cells overlapped with the nucleus. (Scale bars: 10 μm, *A*; 5 μm, *C* and *E*.)

the LIS1 function in nuclear migration (Fig. 6*E*). In conclusion, these results suggest that microtubule-based migration of the nucleus and centrosome is differentially regulated by the microtubule-associated dynein motor complex.

Discussion

Previous live imaging studies using several types of migrating neurons have demonstrated that the centrosome leads the nucleus and moves forward coordinately and prompted the hypothesis that microtubule-dependent pulling forces on the nucleus are converged at the centrosome (7, 8, 12, 13, 18). In contrast, our imaging studies revealed nuclear migration past the centrosome, excluding the pulling effect of the centrosome as its major driving force. Our results are supported by previous electron microscopic observations that centrosomes are located to the side of cell bodies in migrating neurons (9, 10). Studies using dissociated granule cells have indicated that small-amplitude movements of the soma (1.3 μm on average) were preceded by centrosomal movements every 3–5 min (7). Although we did not detect high-frequency movements in the present time-lapse analysis at 3-min intervals, such coordinated small-amplitude movements of the nucleus and centrosome might have occurred during slow-moving phases. Nonetheless, our discovery of the fast, long-distance nuclear advances past the centrosome, which were not observed in dissociated cultures, are an important contribution to understanding nuclear migration in the brain.

In contrast to granule cells, the centrosomes in tangentially migrating cortical interneurons and SVZ cells are consistently positioned in front of the nuclei and migrate toward the swelling within the leading processes, indicating the distinct cellular kinetics in differential modes of neuronal migration. However, a previous report has suggested that the nucleus may pass the centrosome in SVZ neuroblasts in culture (33). In addition, it has been suggested that the centrosome is only loosely anchored to microtubules in migrating cortical interneurons and granule cells (18, 34), which brings into question whether the nucleus is constitutively coupled to the centrosome by perinuclear microtubules during neuronal migration. The forward migration of the centrosome is correlated with extension of a long leading process (up to 150 μm length) in cortical interneurons (18). Because cortical interneurons migrate at significantly higher speeds than granule cells (37.5–58 μm/h compared with 17.1 ± 2.4 μm/h in granule cells) (18, 35), the movement of the centrosome far in advance of the nucleus might be led by rapid extension of the long leading process in these cells. Furthermore, most recent evidence supports that the motion kinetics of the nucleus and centrosome are independent of each other in radially migrating neural precursors in organotypic slices of developing rat neocortex (36). Thus, albeit apparent differences in migration kinetics, the centrosome might not be directly involved in driving the microtubule-dependent translocation of the nucleus even in neurons whose centrosome maintains a position ahead of the nucleus.

Although our results disprove the pulling effect of the centrosome, microtubule-dependent nuclear transport is clearly a predominant mechanism for nuclear migration. We identified two distinct types of microtubule structures around the nucleus. One corresponds to the previously identified microtubule cage enveloping the nucleus, which consists of dynamic microtubules. The other is the whisk-like structure which is composed of stable microtubules and extends from the leading process toward the anterior surface of the nucleus. Neither structure converged at the centrosome, supporting our finding that the centrosome does not exert a pulling force on the nucleus. Specific disruption of dynamic microtubules failed to inhibit nuclear migration, whereas loss or excess formation of stable microtubules halted nuclear migration. This finding suggests that polarized formation and dynamic rearrangement of the nucleus-associated stable microtubules is crucial for nuclear migration. In contrast to the perinuclear microtubule structures in the cell bodies that diverged from the centrosome, the stable microtubule bundles within the leading process appeared to be tightly coupled to the centrosome. The coupling of the centrosome and microtubule bundles within the leading process was not affected by inhibition of dynein/LIS1 complex function. In contrast, the nucleus was left behind the centrosome in cells overexpressing dominant-negative LIS1, suggesting that the dynein/LIS1 complex exerts the force driving nuclear movement along microtubules (8, 13, 27). Recently, Tsai *et al.* (36) reported that LIS1-dynein disfunction by strong RNAi or the same dominant-negative LIS1 (LIS1N) used in this study blocked both nuclear and centrosomal migration. In contrast, partial knockdown of LIS1 induced similar

phenotypes to our present observation and selectively disrupted nuclear migration. It is thus possible that the dominant inhibitory effect of LIS1N was partial and selectively disrupted nuclear migration in our experimental conditions. Nonetheless, our present findings are consistent with their conclusion that LIS1/dynein complex regulates nuclear movement independently of centrosomal positioning.

We believe that the centrosome is positioned ahead of the nucleus and integrates the microtubule structures during resting phases; the perinuclear microtubules are rapidly released from the centrosome once they are nucleated. In the moving phase, the nucleus translocates along the polarized noncentrosomal microtubules regardless of the position of the centrosome; the LIS1/dynein complex at the nuclear membrane would be responsible for transporting the nucleus by its microtubule-based motor activity (8, 13). Nuclear migration might require additional driving forces such as nonmuscle myosin II-dependent actomyosin contractility (12, 18, 36). The centrosome moves along microtubule bundles toward the leading process independently of the nuclear movement and regains its position ahead of the nucleus (SI Fig. 10*C*). Dynamic microtubule-organizing activity of the centrosome has recently been demonstrated in migrating neural precursors (36). Thus, the positioning of the centrosome in front of the nucleus during the resting phase might be important for the polarized arrangement of the microtubules for the next cycle of nuclear migration in the resting phase. The mechanisms controlling cell polarity likely regulate centrosome positioning in front of the nucleus to define a polarized shape and directionality in migrating neurons (4, 7, 33, 37).

Materials and Methods

DNA Constructs. For expression in granule cells at moderate levels, the molecules of interest were subcloned into a pCAGGS expression vector (38). Details are described in *SI Text*.

***In Vivo* Electroporation.** P8 ICR mice were anesthetized on ice. The occipital skin and muscles were cut open, and a small incision was made in the bone over the cerebellum with a 27-gauge needle. Six micrograms of plasmid DNA mixed at 1:1 was solved in 1 μl of Tris-EDTA buffer containing 0.1% fast green and injected through the incision with a microsyringe with a 33-gauge needle (Ito, Shizuoka, Japan), which was connected to the anode of a pulse generator. After injection, tweezer-type electrodes connected to the cathode were placed on the occipital regions, and electric pulses (six pulses of 70 mV for 50-ms duration with 150-ms intervals) were applied by using a pulse generator, CUY21 (Nepagene, Chiba, Japan). After the wound was sutured, the pups were revived at 37°C and returned to the litter. Nuclear staining and immunostaining of the transfected cells in tissue after *in vivo* electroporation were performed as described in *SI Text*.

Time-Lapse Imaging. Cerebella were dissected and embedded in 3% agarose 2 days after electroporation and sectioned into 300-μm-thick coronal slices by using a vibratome (linear slicer PRO 7, Dosaka EM, Kyoto, Japan). Slices were placed on a Millicell-CM plate (Millipore, Bedford, MA), mounted in collagen gel, and soaked in culture medium (15% heat-inactivated horse serum, 25% Earle's balanced salt, 60% Eagle's basal medium, 5.6 g/liter glucose, 3 mM L-glutamine, 1.8 mg/ml $NaHCO_3$, 1 mM sodium pyruvate, 5 μg/ml bovine insulin, 5 μg/ml human transferrin, 30 nM sodium selenite, and 20 nM progesterone). Slices in Millicell-CM dishes were kept at 37°C in an incubator chamber attached to an upright microscope stage (BX61WI; Olympus, Tokyo, Japan) and provided with constant gas flow (85% O_2, 5% CO_2, 10% air). After slices were allowed to settle for 2–4 h, time-lapse images were obtained with a laser scanning confocal microscope (FV1000; Olympus). Centrosome kinetics were viewed through a ×60 water-immersion objective (numerical aperture 1.10; Olympus). All other images were viewed through a ×20 water-immersion objective (numerical aperture 0.50). Ten to 20 optical Z sections at 10 μm (×20 objective) or 2 μm (×60 objective) steps were obtained and stacked to acquire whole images. Quantitative analysis of time-lapse data were performed with ImageJ software (http://rsb.info.nih.gov/ij/index.html).

Cerebellar Reaggregate Culture. Reaggregate cultures of cerebellar external granule layer cells were performed as described with a few modifications (16). Time-lapse imaging and immunostaining of reaggregate cultures were performed as described in *SI Text*.

We thank Y. Matsubayashi for invaluable advice and R. T. Yu for critical reading of the manuscript. This work was supported by grants from the Ministry of Education, Culture, Sports, Science, and Technology of Japan (to M.K.).

1. Hatten ME (2002) *Science* 297:1660–1663.
2. Edmondson JC, Hatten ME (1987) *J Neurosci* 7:1928–1934.
3. Lambert de Rouvroit C, Goffinet AM (2001) *Mech Dev* 105:47–56.
4. Ridley AJ, Schwartz MA, Burridge K, Firtel RA, Ginsberg MH, Borisy G, Parsons JT, Horwitz AR (2003) *Science* 302:1704–1709.
5. Komuro H, Rakic P (1998) *J Neurosci* 18:1478–1490.
6. Rivas RJ, Hatten ME (1995) *J Neurosci* 15:981–989.
7. Solecki DJ, Model L, Gaetz J, Kapoor TM, Hatten ME (2004) *Nat Neurosci* 7:1195–1203.
8. Tanaka T, Serneo FF, Higgins C, Gambello MJ, Wynshaw-Boris A, Gleeson JG (2004) *J Cell Biol* 165:709–721.
9. Rakic P (1972) *J Comp Neurol* 145:61–83.
10. Gregory WA, Edmondson JC, Hatten ME, Mason CA (1988) *J Neurosci* 8:1728–1738.
11. Xie Z, Sanada K, Samuels BA, Shih H, Tsai LH (2003) *Cell* 114:469–482.
12. Schaar BT, McConnell SK (2005) *Proc Natl Acad Sci USA* 102:13652–13657.
13. Tsai LH, Gleeson JG (2005) *Neuron* 46:383–388.
14. Metin C, Baudoin JP, Rakic S, Parnavelas JG (2006) *Eur J Neurosci* 23:894–900.
15. Rakic P (1971) *J Comp Neurol* 141:283–312.
16. Kawaji K, Umeshima H, Eiraku M, Hirano T, Kengaku M (2004) *Mol Cell Neurosci* 25:228–240.
17. Komuro H, Rakic P (1995) *J Neurosci* 15:1110–1120.
18. Bellion A, Baudoin JP, Alvarez C, Bornens M, Metin C (2005) *J Neurosci* 25:5691–5699.
19. Rios RM, Bornens M (2003) *Curr Opin Cell Biol* 15:60–66.
20. Higginbotham HR, Gleeson JG (2007) *Trends Neurosci* 30:276–283.
21. Gundersen GG, Khawaja S, Bulinski JC (1987) *J Cell Biol* 105:251–264.
22. Bulinski JC, Richards JE, Piperno G (1988) *J Cell Biol* 106:1213–1220.
23. Ahmad FJ, Pienkowski TP, Baas PW (1993) *J Neurosci* 13:856–866.
24. Brown A, Li Y, Slaughter T, Black MM (1993) *J Cell Sci* 104:339–352.
25. Baas PW, Black MM (1990) *J Cell Biol* 111:495–509.
26. Baas PW, Slaughter T, Brown A, Black MM (1991) *J Neurosci Res* 30:134–153.
27. Shu T, Ayala R, Nguyen MD, Xie Z, Gleeson JG, Tsai LH (2004) *Neuron* 44:263–277.
28. Tsai JW, Chen Y, Kriegstein AR, Vallee RB (2005) *J Cell Biol* 170:935–945.
29. Wynshaw-Boris A, Gambello MJ (2001) *Genes Dev* 15:639–651.
30. Tai CY, Dujardin DL, Faulkner NE, Vallee RB (2002) *J Cell Biol* 156:959–968.
31. Nasrallah IM, McManus MF, Pancoast MM, Wynshaw-Boris A, Golden JA (2006) *J Comp Neurol* 496:847–858.
32. Echeverri CJ, Paschal BM, Vaughan KT, Vallee RB (1996) *J Cell Biol* 132:617–633.
33. Higginbotham H, Tanaka T, Brinkman BC, Gleeson JG (2006) *Mol Cell Neurosci* 32:118–132.
34. Baird DH, Myers KA, Mogensen M, Moss D, Baas PW (2004) *Neuropharmacology* 47:677–683.
35. Polleux F, Whitford KL, Dijkhuizen PA, Vitalis T, Ghosh A (2002) *Development (Cambridge, UK)* 129:3147–3160.
36. Tsai JW, Bremner KH, Vallee RB (2007) *Nat Neurosci* 10:970–979.
37. de Anda FC, Pollarolo G, Da Silva JS, Camoletto PG, Feiguin F, Dotti CG (2005) *Nature* 436:704–708.
38. Niwa H, Yamamura K, Miyazaki J (1991) *Gene* 108:193–199.